Wasit Journal of Engineering Sciences

Journal homepage: https://ejuow.uowasit.edu.iq

Efficient Dye Removal and Water Treatment Feasibility Assessment for Iraq's Industrial Sector: A Case Study on Terasil Blue Dye Treatment Using Inverse Fluidized Bed and Adsorption

Sadiq Mussadaq M Baqer[1], Hatem A Gzar[1],Mahdi Nuhair Rahi[1], and Qasim M Jani[1]

Affiliation
[1]Civil Engineering Department College of Engineering, Waist University
Waist , Iraq

Correspondence
Sadiq Mussadaq M Baqer
Email:
engsadiqalhakeem32@gmail.com

Received
29-December-2023
Revised
31-January-2024
Accepted
14-February-2024

Doi:

Abstract

In this study, we investigated Terasil blue dye absorption on modified rice husk through batch and continuous trials. In continuous mode includes experimental tests in an inverse fluidized bed teqnique at various times and under various operating conditions (bed height, initial concentration, and varying flow rate) were investigated. The effect of various factors like pH, contact time, agitation speed and particle size on the removal efficiency (%) the Terasil blue dye were thoroughly investigated. The maximum removal efficiency (%) was achieved up to pH 7.0. Removal efficiency (%) increased with increasing contact time. The maximum removal efficiency (%) was achieved at 200 RPM (rate per minute). Increasing in the particle size caused decreased in the removal efficiency (%). In batch experiments the Freundlich, and Temkin models showed good agreement with R^2 value while the Langmuir model had moderate agreement. The value of qe is 1.73 mg/g under specific conditions; the Langmuir model provides q-max of 0.0078 mg/g and K-L of 0.0801 L/mg.Ongoing tests conducted in an inverse fluidized bed offer valuable insights into the hydrodynamic behavior of the system.

The collected data effectively demonstrates the variations in pressure drops and bed heights. There is a positive correlation between bed height and fluid velocity, suggesting a significant association within the dynamics of fluidized beds.

These experimental results by combining with computational data will offer deep insight to the phenomena of adsorption and will provide practical applications for enhancing the efficiency of adsorption system in the fields of environmental and chemical engineering.

Keywords: Rice husks, Hydrodynamics, Fluidization velocity, and Artificial Neural Network (ANN).

الخلاصة:

في هذه الدراسة، بحثنا امتصاص صبغة تيراسيل الزرقاء على قشور الأرز المعدلة من خلال تجارب الدفعات والتجارب المستمرة. يتضمن الوضع المستمر اختبارات تجريبية في تقنية الطبقة المميعة العكسية في أوقات مختلفة وتحت ظروف تشغيل مختلفة (ارتفاع الطبقة المميعة، التركيز الأولي، ومعدل التدفق المتغير). تم التحقيق بدقة في تأثير عوامل مختلفة مثل درجة الحموضة، وزمن التلامس، وسرعة التحريك، وحجم الجسيمات على كفاءة الإزالة (%) للصبغة التيراسيل الزرقاء. تم تحقيق أقصى كفاءة إزالة (%) حتى درجة الحموضة 7.0. زادت كفاءة الإزالة (%) مع زيادة وقت التلامس. تم تحقيق أقصى كفاءة إزالة (%) عند 200 دورة في الدقيقة. أدى زيادة حجم الجسيمات إلى انخفاض في كفاءة الإزالة.(%) في تجارب الدفعات، أظهرت نماذج فرويندليش وتمكين توافقًا جيدًا مع قيمة R^2 بينما أظهر نموذج لانغمير توافقًا معتدلًا. تبلغ قيمة سعة

الامتصاص التوازني (qe) 1.73 ملغم / جم تحت ظروف محددة؛ يوفر نموذج لانغمويز 0.0078 q-max ملغم / جم و 0.0801K-L لتر / ملغم. تقدم التجارب المستمرة التي أجريت في الطبقة المميعة العكسية رؤى قيمة حول السلوك الهيدروديناميكي للنظام. توضح البيانات المجمعة بشكل فعال الاختلافات في انخفاض الضغط وارتفاعات الطبقة. هناك علاقة تامة الإيجابية بين ارتفاع الطبقة وسرعة السائل، مما يشير إلى ارتباط كبير داخل ديناميكيات الطبقات المميعة.
ستقدم هذه النتائج التجريبية بالاشتراك مع البيانات الحسابية رؤى عميقة حول ظاهرة الامتصاص وستوفر تطبيقات عملية لتعزيز كفاءة نظام الامتصاص في مجالات الهندسة البيئية والكيميائية.

1. INTRODUCTION

This study explains the hydrodynamic characteristics and applications of liquid-solid inverse fluidization in various configuration like sloped walls or tapering top section. Inverted fluidized reactors have vast applications in oil water separation, biofilm cultivation, and reduction of COD, BOD, TOC levels. The minimum "fluidization" is crucial and depends on the fluid flow system's elements and characteristics [1, 2].

Water stands as a fundamental element supporting all life on our planet, underscoring its unparalleled importance [3]. Nonetheless, the escalating challenges of global water contamination have become increasingly urgent, fueled by rapid industrialization, population growth, and climate change [4]. A stark forecast suggests that by 2025, freshwater scarcity could affect up to 50% of the world's population, surging to a staggering 75% by 2075 [5]. Pollution due to industrial discharge and urban activities creates hazardous contaminants, which lead to human health risk and disturbing ecosystems. The significance of wastewater treatment looms large, particularly in sectors like textiles, notorious for their substantial water consumption and pollution footprint. To put it into perspective, a mere 0.5 kg of textile products demands a staggering 80 L of water [6]. Disturbingly, the textile industry alone accounts for the direct release of 2% of all dyes into aquatic ecosystems, posing both health and environmental risks [7, 8].

In inverse fluidized bed reactor with three phases hydrodynamics promote solid fluid fluidization. Fluidization mainly depend upon gas's larger diameter. In this method the breakdown of wastewater depend largely on treatment duration, gas velocity, height-to-width ratio and settled waste volume to treatment area volume (V_b/V_r) [15]. The three phases hydrodynamics had a lower minimum fluidization voidage than two-phase structure. The wetting agent had great impact on performance of inverse fluidized bed reactor as it decrease the minimum fluidization velocity [16]. The rectangular three-phase "inverse fluidized bed" investigation discovered that temperature directly influences bed voidage or heat transfer coefficient. Bed voidage, gas velocity, and fluid velocity promote heat transmission [17-19].

In the current study, modified rice husks as an adsorbent was developed. The modified rice husks is then employed as an adsorbent in inverse fluidized bed reactors which can present an eco-friendly and cost-effective approach to wastewater treatment. The modified rice husks was then utilized to remove Terasil blue dye. In this study, both batch and continuous trials were used. The hydrodynamic behavior of the modified rice husk in inverse fluidized beds was also investigated. This research also investigate correlations between fluid velocity, pressure drops, and bed heights. The effect of various factors like pH, contact time, agitation speed, particle size, adsorbent dosage on the dye removal efficiency(%) were also investigated. Different adsorption models like Langmuir, Freundlich and Temkin were also employed to deeply investigate the kinetics of dye adsorption. This insight contributes to optimizing the efficiency of the proposed wastewater treatment method for practical applications.

2. METHODS AND MATERIALS

2.1. Method: Research Design

This research study mainly concentrates on the development of an adsorbent created from modified risk husks for efficient removal of Terasil blue dye from industrial wastes utilizing inverse fluidized bed reactor. This investigation focuses on the influence of various parameters like pH, contact time, agitation speed, particle size

and adsorbent mass on the removal efficiency (%) of the Terasil blue dye. Different adsorption models like Langmuir, Freundlich and Temkin mainly focus on the kinetics of adsorption process. This study include detail setup of the experimental setup for the development of modified rise husks and their employment as adsorbent for the removal of Terasil blue dye. This study also include sampling procedures and data collection using statistical tools. Data analysis will be carried out using help of figures and tables. The discussion will be for the interpretation of results, comparing of results with literature findings and future practical applications. The conclusion of this study will be brief summarization of the key findings, exploring significance of the results and future implications.

2.2. Preparation

To evaluate the color intensity and behavior of Terasil blue dye, a spectral analysis was performed. The absorbance or transmittance properties of the dye solution were measured across a range of wavelengths using a UV-Vis spectrophotometer. This analysis provided insights into the dye's optical characteristics and aided in determining its initial color density. A sample was collected and centrifuged at each time point, and the remaining concentration of adsorbed dye in the fluid stage was acquired after 5 minutes of centrifuging. To determine the quantity of dye adsorbed by rice husk powder, the starting and last dye concentrations in the aqueous solutions were measured, and the changes were calculated.

2.3. Batch Experiment Study

Experimental work on terasil blue dye adsorption using rice husk as the adsorbent was conducted in batch mode, varying parameters such as pH, temperature, dose level, metal ion concentration, and contact time. Optimal adsorption conditions were determined by adjusting pH (3.0 to 7.0 at 25°C) with a starting dye concentration of 40 mg/L in a 120 mL solution. The higher dye concentration aimed to minimize variability in results, ensuring efficient adsorption and reproducibility in the experimental work. The contact time of 60 minutes was kept with a rice husk powder quantity of 0.5-2.5 g/L. The experiment system was continuously stirred for 60 minutes to ensure achieving the equilibrium.

2.4. Kinetic and Adsorption Study

The adsorption of terasil blue dye onto rice husks can be modeled using a variety of different models. One common model is the Langmuir isotherm, which assumes that the adsorption of dye onto the rice husks is a reversible process that follows a linear relationship. Experiments were conducted to investigate equilibrium isotherms for optimizing the design of the Terasil blue dye removal system from wastewater. These investigations was based on data obtained from the adsorbent dose study.

2.5. Statistical analysis

The Model is based on ANN (ANN network) as well as SPSS through the parameters extracted from the practical and not only on the rice husks. A comparison is made between the three (practical, ANN and SPSS) and optimization selection. There are a number of other models that can be used to describe the adsorption of terasil blue dye onto rice husks. The choice of model depends on the specific experimental conditions and the desired level of accuracy.

3. Results and Discussion

3.1. Removal Efficiency (%) of the modified rise husks

The study found that the adsorption capacity of rice husk for Terasil blue dye rises with higher dye concentration and sorbent dosage. The maximum adsorption occurs with activated rice husk at a sorbent dosage of 10.0 g/l and a Terasil blue dye concentration of 25.0 mg/l. The adsorption kinetics aligns with a pseudo-second-order model, suggesting that the process is governed by the diffusion rate of terasil blue dye molecules into the rice husk pores. The removal efficiency (%) of the modified rise husks for the removal of Terasil blue

dye was investigated using different parameters like pH, contact time, agitation speed, particles size.

The effect of pH on the removal of Terasil blue dye with modified rise husks thoroughly investigated. The investigation was made from pH (3 to 9.0) in order to find maximum removal efficiency. As shown in Table 1 and Figure 1 (A) the maximum removal efficiency of 89.58 % was achieved at pH 7. At pH 3, the dye concentration in the solution after adsorption was 5.96 mg/L. Particles absorbed 14.04 mg/L dye, resulting in 70.21% clearance efficiency [20]. The table also shows data for different pH levels, revealing how pH affects adsorption. In general, this data helps researchers determine the best pH settings for color removal using Modified Rice Husk particles. The efficacy of adsorption is affected by the agitation speed; a higher RPM (Rotation Per Minute) leads to better removal. The data as shown in Table 1 displays Modified Rice Husk particle studies to determine the optimal agitation velocity for Terasil blue dye removal. Adsorbent, contact time, temperature, and starting dye concentration were constant in the tests [21]. There are numerous RPM agitation speeds and their effects. The "Agitation Speed (RPM)" column records the solution and adsorbent's spinning rates. The dye concentration in the solution after adsorption is Ce (mg/L). This number falls as agitation speed increases, indicating dye removal efficiency. Under various agitation speeds, the "Amount Absorbed (mg/L)" parameter measures dye elimination and adsorption. At 150-minute contact time concentration of Terasil, blue dye was 7.74 mg/L. The levels dropped to 4.51 mg/L after 180 minutes. The lowest concentration (2.48 mg/L) of dye achieved at 200 minutes contact time, which is the maximum removal efficiency of the adsorbent. Similarly, dye adsorption onto particles increased proportionally, increasing removal efficiency. An estimated 61.32% of the dye was removed after 150 minutes. System efficiency increased to 77.47% after 180 minutes and 87.59% at 200 minutes [24]. Removal efficiency was 84.87% at 210 minutes. The solution's dye concentration decreased during the experiment. This concentration drop shows that Rice Husk particles removed the color. The removal effectiveness is better for larger particles. The Rice Husk particles have proven effective as adsorbents for this purpose. Particles between 1.18 and 2 mm had 94.10% dye clearance efficiency. At 3.35-4.25 mm, particles were 90.20% efficient, whereas at 2-3.35 mm, they were 92.3% efficient. The above percentages show how well different particle sizes remove Terasil blue color from water. This data Table 1 and Figure 1 (D) helps scientists choose the best particle size for practical applications, ensuring dye removal from contaminated water sources [25] Another important factor is the adsorbent mass; at greater concentrations and masses, the removal effectiveness may reach as high as 97.15 per cent. The results provide light on how to maximize dye adsorption efficiency.

Table 1**:** Effect of different factors on the adsorption of Terasil blue dye onto Modified Rice Husk particles

pH	**Ce (mg/L)**	**Amount Absorbed (mg/L)**	**Removal Efficiency (%)**
3	5.96	14.04	70.21
4	4.64	15.36	76.78
5	4.02	15.98	79.92
6	3.77	16.23	81.46
7	**2.08**	**17.92**	**89.58**
8	2.28	17.72	88.61
9	2.25	17.75	88.74
Agitation speed (RPM)	**Ce (mg//L)**	**Amount Absorbed (mg/L)**	**Removal Efficiency (%)**
125	2.68	17.32	86.62
150	2.02	17.98	89.91
200	**1.55**	**18.45**	**92.23**

250	1.63	18.37	91.92
Time (min)	**Ce (mg/L)**	**Amount Absorbed (mg/L)**	**Removal Efficiency (%)**
120	11.88	8.12	40.6
159	7.74	12.26	61.32
180	4.51	15.49	77.47
200	**2.48**	**17.52**	**87.59**
210	0.03	16.97	84.87
Adsorbent Mass (g)	**Ce (mg/L)**	**Amount Absorbed (mg/L)**	**Removal Efficiency (%)**
0.5	11.34	8.66	56.72
1	12.55	7.45	62.74
2.00	14.87	5.13	74.36
3.00	18.74	1.26	93.70
4.00	**19.43**	**0.57**	**97.15**
Particle Size (mm)			**Removal Efficiency (%)**
1.18_2			**94.10**
2-3.35			92.3
3.35-4.25			90.20

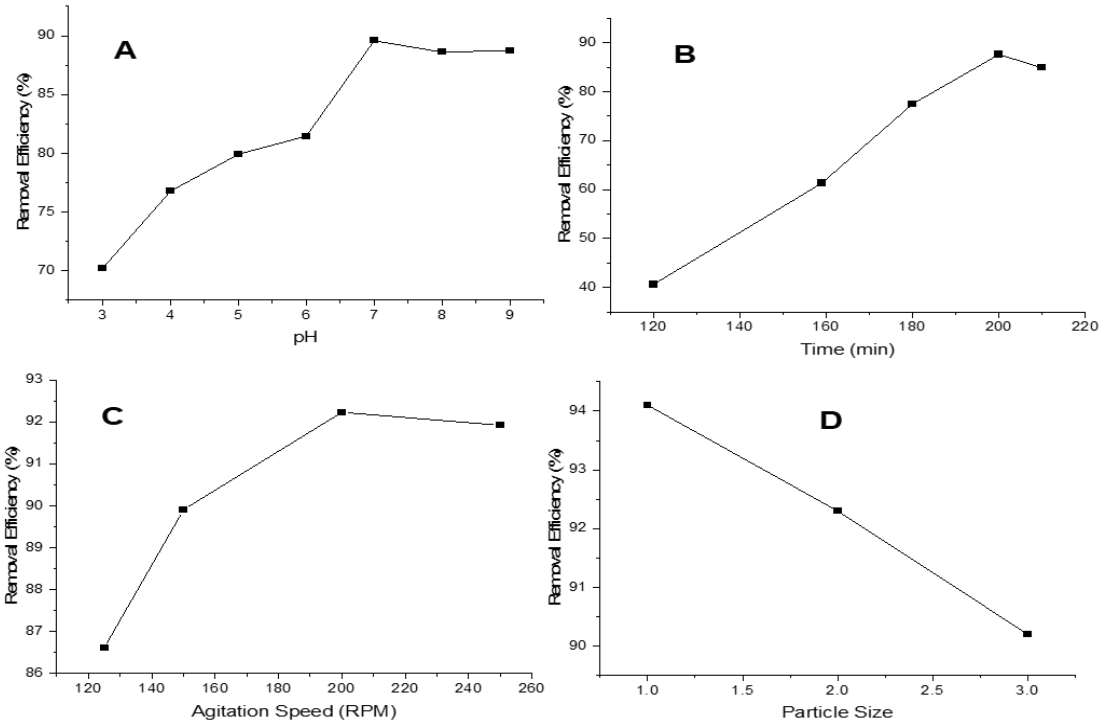

Fig. 1 Effect of various factors on removal efficiency (%) of Terasil blue dye adsorption on Modified Rice Husk particles **(A)** pH **(B)** Time **(C)** Agitation speed **(D)** Particle size

3.2. Comparative investigation of current and previous adsorption models

Table 2 compares the current and previous models' removal effectiveness for varied adsorbent masses (W) and Terasil blue dye concentrations. The present model outperforms its predecessor in terms of removal efficiency in every single instance. For example, the removal effectiveness is 56.72% in the new model, up from 46% in the prior model, for a mass of 0.5 g and a concentration range of 11.34-13.50 mg/L. This trend holds for more mass-concentration pairings, further demonstrating that the present approach consistently achieves better removal efficiency under different circumstances.

Table 2**:** Comparison for removal efficiency by current and previous model

W(g)	**Concentration(mg/l)**	**Removal(%) by current model**	**Removal(%) by Previous model**
0.5	11.34-13.50	56.72	46
1	12.55-9.50	62.74	62
2	14.87-6.75	74.36	73
3	18.74-4	93.70	84

3.3. Equilibrium isotherms for adsorption of Terasil blue dye

Adsorbent concentration (g/L) is the amount of rice husk dissolved in one litre of water, showing its density. The concentration of terasil blue dye is presented as in mg/L of water. The rate constant K (min^-1) measures the adsorption process in minutes raised to the power of minus one. An increased rate constant means more adsorption [26]. A statistical indicator called the "r value" measures experimental data-theoretical model agreement. A correlation coefficient (r) around 1 implies a strong relationship between observed and anticipated values. Using activated rice husk at 5.0 g/l adsorbent and 5 mg/l dye, the first experiment yielded a rate constant (K) of 0.013 min^-1 and a r value of 0.90. The model fits well with this r-value [27]. The table shows data on different quantities of adsorbents and dye, allowing researchers to compare the terasil blue dye adsorption of untreated and citric acid-treated rice husks. These insights are important for practical applications, especially where water dye and pollution removal are crucial. The column shows the solution's original terasil blue dye concentration. At equilibrium, Qe is the amount of dye adsorbed per unit mass of adsorbent [2]. The Ce/Qe column shows the quotient of the original dye concentration by the equilibrium dye adsorption. The logarithm of the dye's initial concentration is "log (Ce)". The column shows the solution's original terasil blue dye concentration. At equilibrium, Qe is the amount of dye adsorbed per unit mass of adsorbent. The Ce/Qe column shows the quotient of the original dye concentration by the equilibrium dye adsorption. The logarithm of the dye's initial concentration is "log (Ce)". Adsorption occurs when molecules of a substance connect to the surface of a solid [28].

Table 3: Data for Langmuir, Freundlich and Temkin Adsorption models

C_e	q_e	C_e/Q_e	$log\ c_e$	$log\ q_e$	$ln\ c_e$

11.34	1.73	6.555	1.05	0.24	
12.55	0.75	16.73	1.99	-0.125	2.53
14.87	0.25	59.48	1.172	-0.602	2.7
18.74	0.042	449.19	1.273	-1.376	2.93
19.43	0.015	1295.33	1.29	-1.824	2.967

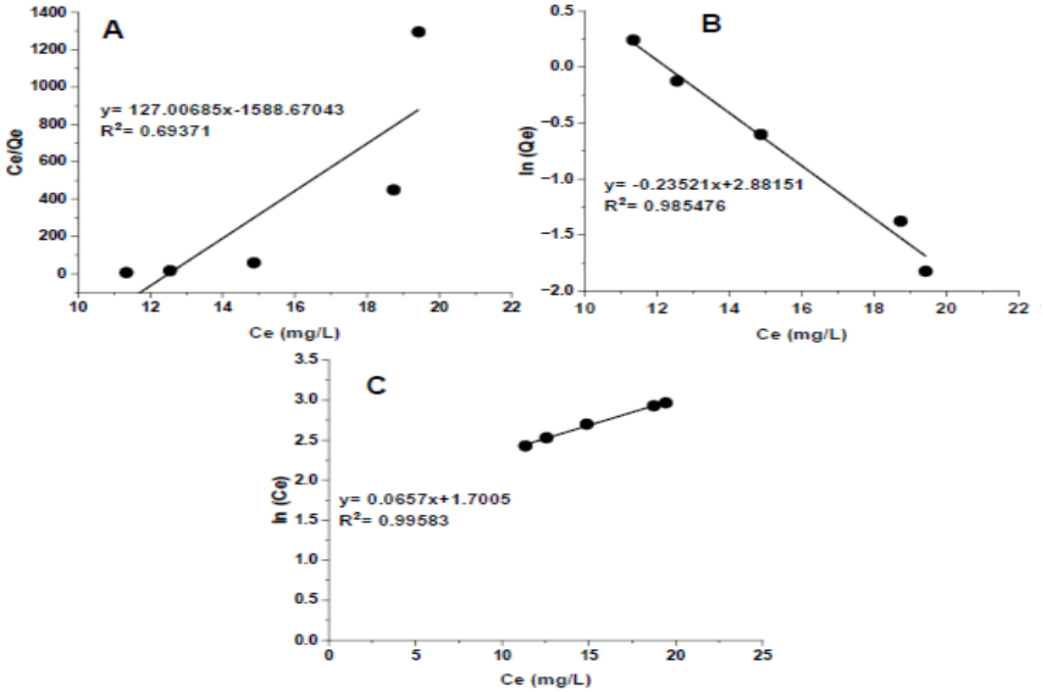

Fig. 2 Different adsorption models for Terasil blue dye **(A)** Langmuir **(B)** Freundlich and**(C)** Temkin models

3.4. Effect of pressure drop and bed height on the fluid velocity

Figure 3 displays pressure drop (ΔP) data for masses of 0.04 kg and 0.06 kg at different velocities and bed heights. The "Superficial fluid velocity U (m/s)" represents fluid flow, whereas "Bed Height 10 (cm) Mass of 0.04 (kg)" and "Bed Height 20 (cm) Mass of 0.06 (kg)" reflect experimental circumstances. From this data, Figure 3 may show the link between bed height and surface fluid velocity, revealing system fluid dynamics. Pressure drop data helps explain system behavior at varied velocities and bed heights.

Pressure decreases and rises with fluid velocity. This suggests that when fluid velocity rises in the Rice husk particle bed, flow resistance increases, raising pressure drop. In fluid dynamics and engineering, this connection helps scientists and engineers understand how factors like particle size and fluid velocity affect fluid dynamics in various systems. By studying these patterns, researchers may create safer, more efficient systems for operations like filtration and fluidized bed reactors [29]. The offered information describes an experiment to determine the relationship between inverse fluidized bed height and fluid velocity. The experiment used 1.18–2 mm particles. Bed height rises with fluid velocity, showing a positive association. This knowledge is valuable in chemical engineering because it helps explain fluid-solid interaction dynamics, which are crucial to many processes and applications.

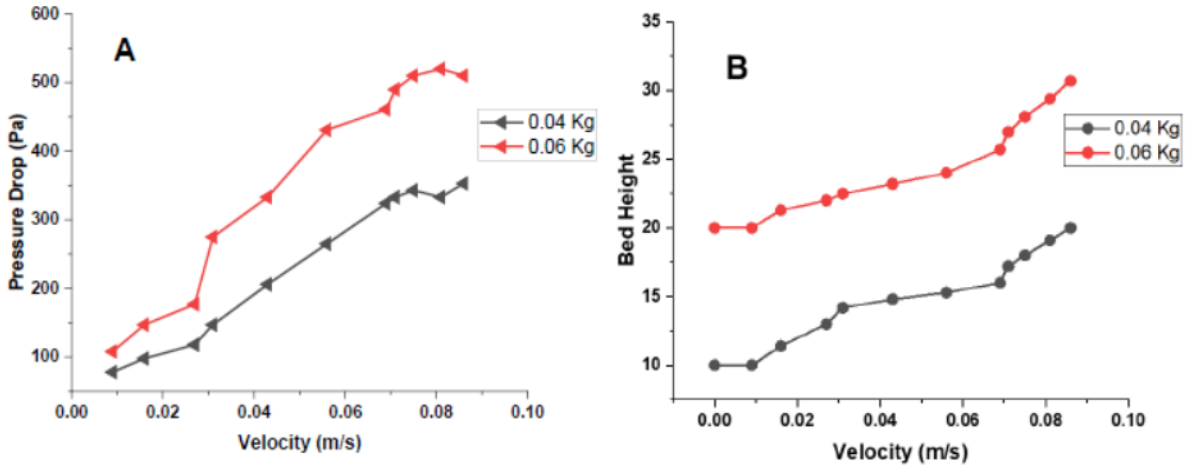

Fig. 3 Superficial fluid velocity vs **(A)** Pressure drop and **(B)** Bed height

Figure 4 shows the adsorption of a chemical over time at different concentrations, bed heights (L), and flow speeds. The data show concentration (C) and ratio of C to beginning concentration (C/Co) with time. From these data, Figure 4 may show how adsorption bed height affects the process. The data helps optimize system adsorption by showing how bed height affects substance adsorption

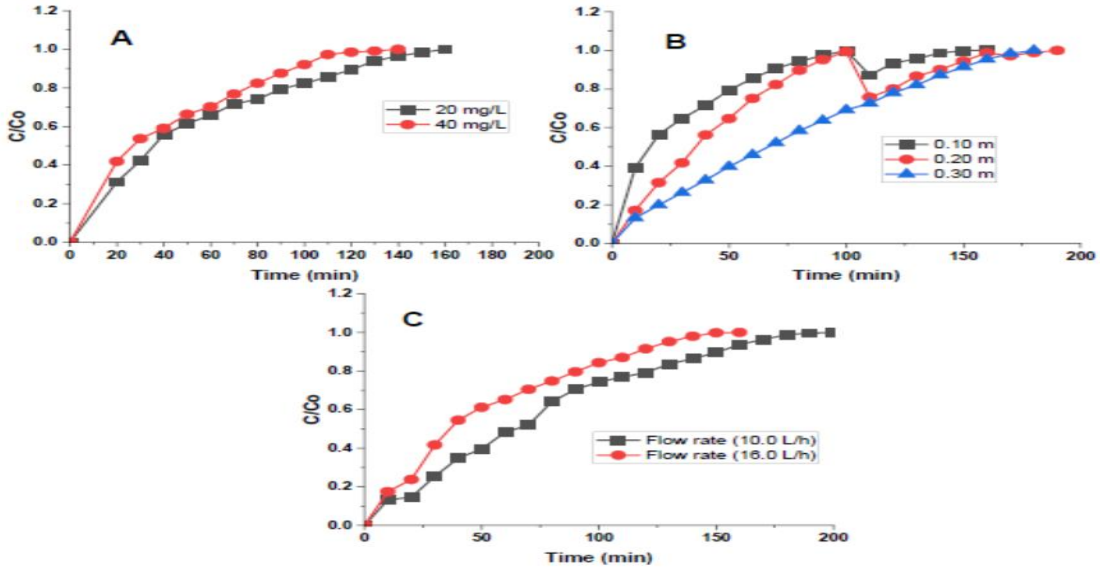

Fig. 4 Adsorption data at **(A)** different initial concentration, **(B)**different bed height and **(C)** Flow rate

Figure 5 shows trials comparing real removal efficiency (RE) to ANN model predictions. Different experiments are in each row. The "Actual RE (%)" column provides the observed removal efficiency, whereas the "Predicted RE (%)" column gives the ANN model's prediction. Root Mean Square Error measures model accuracy in the "RMSE (%)" column. Figure 5, created using this data, and presumably shows the ANN model's experimental outputs, showing its ability to forecast removal efficiency for various tests. This code uses a simple Artificial Neural Network (ANN) model to teach the computer to find patterns in data. Consider the data as a large book with pages for each trial. Starting with data organization is the first step. A virtual robot called the Artificial Neural Network (ANN) model, is then created and supplied with structured data. These situations teach the robot how pH levels and particle sizes affect substance clearance. Learning involves seeing exemplars and understanding linkages [30].

.

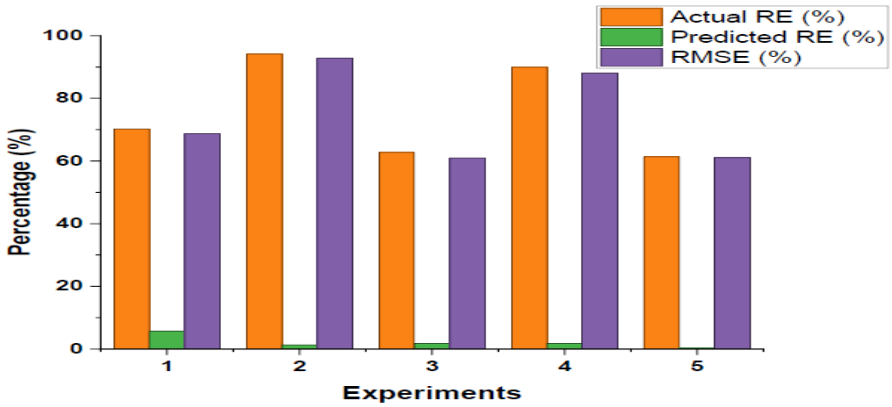

Fig. 5 Experimental Outputs from the ANN Model

Table 4 displays experimental data for two sets with target values, fitted values, and actual data points. Figure 6, constructed from the data, is likely a representation of the experimental data with parameters prediction, illustrating how well the fitted values align with both the target and actual data points. The figure provides a visual comparison of the model's predictions against the observed data, offering insights into the accuracy and performance of the model in capturing the underlying patterns and relationships in the experimental data.

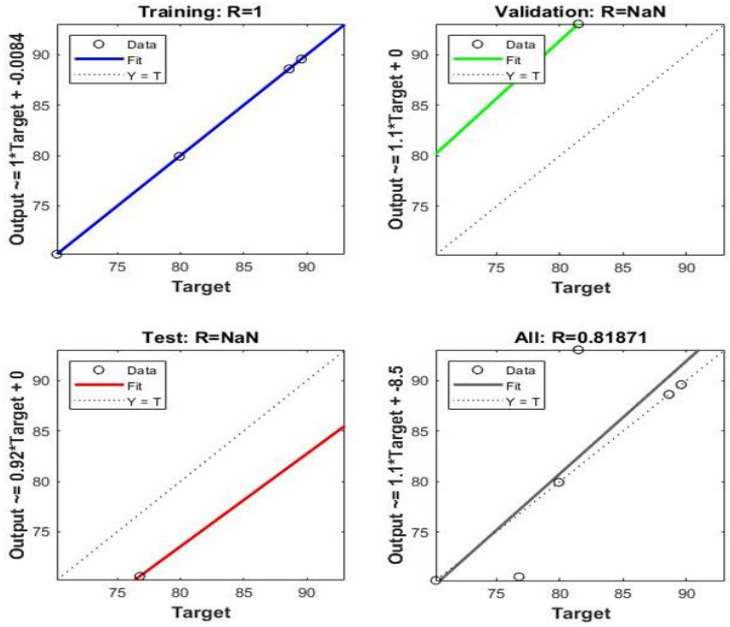

Fig. 6 Experimental data with parameters prediction

Figure 7, the regression model clearly shows that the target, 100 epoches, the target get fit with the data at the All data portion where the RMSE is 0.8187% and this is the least value that get.

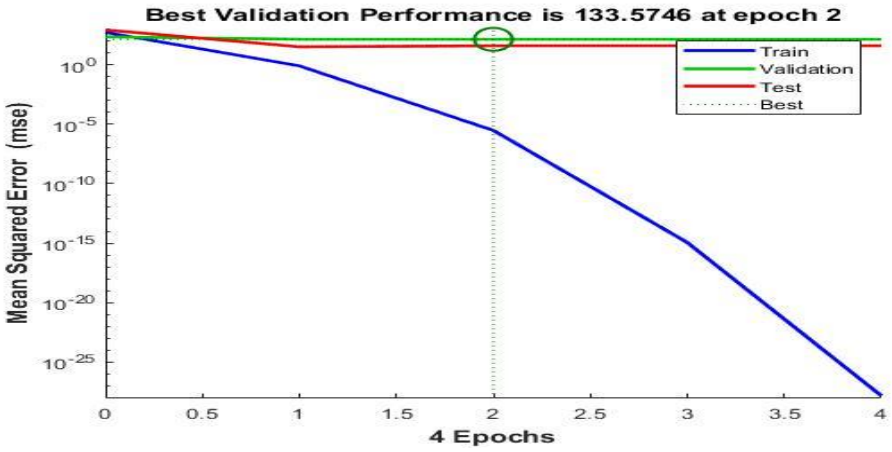

Fig. 7 Overall Performance of the output plot

Table 4**:** Comparison Model of ANN with RSM

Experiments	**Artificial Neural Network**		**Response Surface Methodology**	
	Actual ANN (%)	Predicted RMSE (%)	Actual RSM (%)	Predicted RMSE (%)
Bed Expansion	68.67	0.60	86.87	0.1
Pressure Drop	92.78	0.88	2643.69	1.7

4. CONCLUSION

The comprehensive investigation of the adsorption of Terasil blue dye onto rice husk that has been changed, including several experimental approaches such as batch, continuous, and predictive modelling, provides significant knowledge regarding the complex mechanisms involved in this adsorption phenomenon. The numerical values obtained from experimentation, along with their observed fluctuations, play a crucial role in enhancing our understanding of adsorption mechanisms. Furthermore, these findings have practical significance for applications in environmental and chemical engineering. The present study has yielded significant findings about the adsorption of Terasil blue dye onto modified rice husk. However, there are various potential areas for further investigation and development, which could contribute to a more comprehensive understanding of adsorption processes and improve their practical use.

While the study explores efficient dye removal and water treatment using rice husks in inverse fluidized bed reactors, there is a notable gap in understanding the long-term stability and reusability of the adsorbents. Additionally, the study lacks an in-depth analysis of the economic feasibility and scalability of the proposed wastewater treatment system. Future research should focus on optimizing the regeneration process of the adsorbents to enhance their sustainability and economic viability. Investigating the potential integration of renewable energy sources to power the inverse fluidized bed reactors could further enhance the environmental friendliness of the water treatment system. Moreover, exploring real-world applications and addressing the challenges associated with large-scale implementation would contribute to the practicality of this innovative approach in wastewater treatment.

REFERENCES

1. Ahmaruzzaman M., (2011). Rice Husk and Its Ash as Low-Cost Adsorbents in Water and Wastewater Treatment. Industrial & Engineering Chemistry Research, 13589–13613.
2. Ahmaruzzaman, M., & Gupta, V. K. (2011). Rice Husk and Its Ash as Low-Cost Adsorbents in Water and Wastewater Treatment. *Industrial & Engineering Chemistry Research*, 13589–13613.
3. Gupta, A., Khosla, N., Govindasamy, V., Saini, A., Annapurna, K., Dhakate, S. (2020) Trimetallic composite nanofibers for antibacterial and photocatalytic dye degradation of mixed dye water. Appl. Nanosci. 10, 4191–4205
4. de Oliveira Guidolin, T., Possolli, N.M., Polla, M.B.,Wermuth, T.B., de Oliveira, T.F., Eller, S., Montedo, O.R.K., Arcaro, S., Cechinel, M.A.P. (2021) photocatalytic pathway on the degradation of methylene blue from aqueous solutions using magnetite nanoparticles. J. Clean. Prod. 318, 128556.
5. Zhang, L. (2017) Photocatalysts with Adsorption Property for Dye-Contaminated Water Purification. Bachlor's Thesis, The University of Queensland, Brisbane, Australia.
6. Nuramdhani, I. (2011) Towards Environmentally Benign Wastewater Treatment-Photocatalytic Study of Degradation of Industrial Dyes. Master's Thesis, University of Canterbury, Christchurch, New Zealand.
7. Mohamed, R., Mkhalid, I., Baeissa, E., Al-Rayyani, M. (2012) Photocatalytic degradation of methylene blue by Fe/ZnO/SiO2 nanoparticles under visible light. J. Nanotechnol. 329082.
8. Akpan, U.G., Hameed, B.H. (2009) Parameters affecting the photocatalytic degradation of dyes using TiO2-based photocatalysts: A review. J. Hazard. Mater. 170, 520–529.
9. Al-Ghouti, M. A., Al-Kaabi, M. A., Ashfaq, M. Y., &Da'na, D. (2019). 'Produced water characteristics, treatment and reuse: A review', Journal of Water Process Engineering. Elsevier, pp. 222–239. doi: 10.1016/j.jwpe.2019.02.001.
10. Almaliky, E. A. (2020). 'Geomaterials as cost effective sorbent to remove fluoride from water', Key Engineering Materials, 870, pp. 107–121. doi: 10.4028/www.scientific.net/KEM.870.107.
11. Alvarado-Lassman A, R. E.-A. (2008). Brewery wastewater treatment using anaerobic inverse fluidized bed reactors. BioresourTechnol 99:3009–3015. https://doi.org/10.1016/j.biortech.2007.06.022.
12. Anantharaman A, C. R. ((2018)). Evaluation of correlations for minimum fluidization velocity (Umf) in gas-solid fluidization. Powder Technol 323:454–485. https://doi.org/10.1016/j.powtec.2017.10.016.
13. Aydin S, G. S. (2007). Investigation of using adsorbents obtained from sewage sludge with pyrolysis for removal of cod and dye from textile industry wastewater. Ekoloji 16(64): 43- 48.
14. Azadi, F. S.-J. (2018). 'Experimental Investigation and Modeling of Nickel Removal from Wastewater Using Modified Rice Husk in Continuous Reactor by Response Surface Methodology.
15. Azam, K. S. (2022). A review on activated carbon modifications for the treatment of wastewater containing anionic dyes. Chemosphere, 306, 35566.
16. Banerjee, S. D. (2017). Removal of Basic Dyes from Aqueous Solution by Adsorption Using Rice Husk Ash-A Fixed Bed. International Journal of Advanced Engineering, Management and Science, 3(4).
17. Bayuo, J. P.-B. (2019). Adsorptive removal of chromium(VI) from aqueous solution unto groundnut shell. Applied Water Science, 107.
18. Bayuo, J., Pelig-Ba, K. B., &Abukari, M. A. (2019, May 23). Adsorptive removal of chromium(VI) from aqueous solution unto groundnut shell. *Applied Water Science*, 107.
19. Bi, R. Y. (2022). Efficient removal of Pb(II) and Hg(II) with eco-friendly polyaspartic acid/ layered double hydroxide by host-guest interaction. Applied Clay Science, 225, 106536.
20. C, R. M. (2009). Performance of inverse fluidized bed bioreactor in treating starch wastewater. Front ChemEng China 3:235–239. https://doi.org/10.1007/s11705-009-0020-0.
21. Campos-Díaz K.E., C. J. (2017). Coupled Inverse Fluidized Bed Bioreactor with Advanced Oxidation Processes for Treatment of Vinasse. AIMS Geosciences, 3(4), 538-551.
22. Cho YJ, P. H. (2002)). Heat transfer and hydrodynamics in two- and three-phase inverse fluidized beds. IndEngChem Res 41:2058–2063. https://doi.org/10.1021/ie0108393.
23. Chuah, T. J. (2005). Rice husk as a potentially low-cost biosorbent for heavy metal and dye removal: an overview. Desalination, 175(3), 305-316.
24. Comte MP, B. D. (1997). Hydrodynamics of a three-phase fluidized bed—the inverse turbulent bed. ChemEngSci 52:3971–3977. https://doi.org/10.1016/S0009-2509(97)00240-6.
25. Crini G, L. É.-C. (2018). Adsorption-oriented using conventional and non-conventional adsorbents for wastewater treatment.
26. D., Y. M. (2020). Column adsorption study for the removal of chromium and manganese ions from electroplating wastewater using cashew nutshell adsorbent. Cogent Engineering, 7 (1).
27. El-Said, A. (2010). Biosorption of Pb(II) Io

28. EWC, T. M. (2018). Heat transfer from an immersed tube in a pulsating fluidized bed. ApplThermEng 143:326–339. https://doi.org/10.1016/j.applthermaleng.2018.07.087.
29. EWC, T. M. (2018). Heat transfer from an immersed tube in a pulsating fluidized bed. ApplThermEng 143:326–339. https://doi.org/10.1016/j.applthermaleng.2018.07.087.
30. Fan LS, M. K. (1982). Hydrodynamic characteristics of inverse fluidization in liquid-solid and gas-liquid-solid systems. ChemEng J 24:143–150. https://doi.org/10.1016/0300-9467(82)80029-4.